university of groningen

University Medical Center Groningen

University of Groningen

# Substrate binding tunes the reactivity of hispidin 3-hydroxylase, a flavoprotein monooxygenase involved in fungal bioluminescence

Tong, Yapei; Trajkovic, Milos; Savino, Simone; van Berkel, Willem J H; Fraaije, Marco W

*Published in:*
The Journal of Biological Chemistry

*DOI:*
10.1074/jbc.RA120.014996

**IMPORTANT NOTE: You are advised to consult the publisher's version (publisher's PDF) if you wish to cite from it. Please check the document version below.**

*Document Version*
Final author's version (accepted by publisher, after peer review)

*Publication date:*
2020

Link to publication in University of Groningen/UMCG research database

*Citation for published version (APA):*
Tong, Y., Trajkovic, M., Savino, S., van Berkel, W. J. H., & Fraaije, M. W. (2020). Substrate binding tunes the reactivity of hispidin 3-hydroxylase, a flavoprotein monooxygenase involved in fungal bioluminescence. *The Journal of Biological Chemistry*, *295*(47), 16013-16022. https://doi.org/10.1074/jbc.RA120.014996

**Copyright**
Other than for strictly personal use, it is not permitted to download or to forward/distribute the text or part of it without the consent of the author(s) and/or copyright holder(s), unless the work is under an open content license (like Creative Commons).

The publication may also be distributed here under the terms of Article 25fa of the Dutch Copyright Act, indicated by the “Taverne” license. More information can be found on the University of Groningen website: https://www.rug.nl/library/open-access/self-archiving-pure/taverne-amendment.

**Take-down policy**
If you believe that this document breaches copyright please contact us providing details, and we will remove access to the work immediately and investigate your claim.

*Downloaded from the University of Groningen/UMCG research database (Pure): http://www.rug.nl/research/portal. For technical reasons the number of authors shown on this cover page is limited to 10 maximum.*

JBC Papers in Press. Published on September 11, 2020 as Manuscript RA120.014996
The latest version is at https://www.jbc.org/cgi/doi/10.1074/jbc.RA120.014996

# Substrate binding tunes the reactivity of hispidin 3-hydroxylase, a flavoprotein monooxygenase involved in fungal bioluminescence

Yapei Tong[a], Milos Trajkovic[a], Simone Savino[a], Willem J.H. van Berkel[b], Marco W. Fraaije[a,*]

[a] Molecular Enzymology group, University of Groningen, Nijenborgh 4, 9747AG, Groningen, The Netherlands

[b] Laboratory of Food Chemistry, Wageningen University & Research, Bornse Weilanden 9, 6708 WG, Wageningen, The Netherlands

* corresponding author: M.W. Fraaije
E-mail: m.w.fraaije@rug.nl

M.W. Fraaije: ORCID: 0000-0001-6346-5014
W.J.H. van Berkel: ORCID: 0000-0002-6551-2782
M. Trajkovic: ORCID: 0000-0001-7264-1630
S. Savino: ORCID: 0000-0001-9505-3348

**Running title:** Hispidin 3-hydroxylase from *Mycena chlorophos*

**Keywords:** hispidin, luciferase, hispidin 3-hydroxylase, *Mycena chlorophos*, bioluminescence

Downloaded from http://www.jbc.org/ at University of Groningen on September 15, 2020

**Abstract**

Fungal bioluminescence was recently shown to depend on a unique oxygen-dependent system of several enzymes. However, the identities of the enzymes did not reveal the full biochemical details of this process, as the enzymes do not bear resemblance to those of other luminescence systems, and thus the properties of the enzymes involved in this fascinating process are still unknown. Here, we describe the characterization of the penultimate enzyme in the pathway, hispidin 3-hydroxylase, from the luminescent fungus *Mycena chlorophos* (McH3H), which catalyzes the conversion of hispidin to 3-hydroxyhispidin. 3-Hydroxyhispidin acts as a luciferin substrate in luminescent fungi. McH3H was heterologously expressed in *Escherichia coli* and purified by affinity chromatography with a yield of 100 mg/l. McH3H was found to be a single component monomeric NAD(P)H-dependent FAD-containing monooxygenase having a preference for NADPH. Through site-directed mutagenesis, based on a modeled structure, mutant enzymes were created that are more efficient with NADH. Except for identifying the residues that tune cofactor specificity, these engineered variants may also help in developing new hispidin-based bioluminescence applications. We confirmed that addition of hispidin to McH3H led to the formation of 3-hydroxy-hispidin as sole aromatic product. Rapid kinetic analysis revealed that reduction of the flavin cofactor by NADPH is boosted by hispidin binding by nearly 100-fold. Similar to other class A flavoprotein hydroxylases, McH3H did not form a stable hydro-peroxyflavin intermediate. These data suggest a mechanism by which the hydroxylase is tuned for converting hispidin into the fungal luciferin.

**Introduction**

Bioluminescence is a natural phenomenon in which living organisms emit visible light. Such phenomenon has been observed in a large variety of organisms: fireflies, jellyfishes, bacteria, and fungi. Bioluminescence is often based on a specific precursor molecule, a luciferin substrate, that is converted by a luciferase with concomitant light generation. While fungal bioluminescence has been observed since ancient times (1) and a significant number of luminescent fungi has been described (2), the precise molecular basis for fungal luminescence has remained elusive. All reported luminescent fungi generate the same glow within the emission range of 520−530 nm (3) and are likely to share a bioluminescent system (4). Fungal bioluminescence has attracted the interest of many research groups for a long time (3, 5). Airth and Foerster demonstrated the luciferin-luciferase reaction by mixing fungal extracts and NAD(P)H (6–8). In their work, they suggested that the bioluminescence reaction in fungi is a two-step process involving a NAD(P)H-dependent soluble enzyme and a membrane-bound luciferase (7). The soluble enzyme catalyzes the first step, producing luciferin. In the second step, the luciferase catalyzes the oxidation of the fungal luciferin resulting in light emission. For many decades, no significant progress was made concerning the identification of the fungal luciferin and luciferase system. In 2011, Mori et al. reported that bioluminescence in *M. chlorophos* depends on a specific enzymatic reaction, confirming Airth's work (9). Subsequent work by Teranishi et al. (2016) revealed that part of the bioluminescence system in *M. chlorophos* is localized at the cell membrane (10). Moreover, it was found that *trans*-4-hydroxycinnamic acid and *trans*-3,4-dihydroxycinnnamic acid could increase the light intensity in the living gills of *M. chlorophos* (11, 12), and flavins were likely to be the light emitters in bioluminescence (13). Over the last few years, details on the molecular basis of fungal bioluminescence have emerged. Purtov et al. showed that hispidin is converted to 3-hydroxyhispidin in the presence of molecular oxygen, NAD(P)H, and a hispidin 3-hydroxylase (14). Kaskova et al. (15) clearly illustrated the fungal bioluminescence mechanism in which a luciferase oxidizes 3-hydroxyhispidin into a high-energy intermediate which decays with concomitant light emission. The discovery of the fungal luciferin (3-hydroxyhispidin) biosynthesis and recycling pathway was a breakthrough reported by Kotlobay et al. in 2018 (16). In their study, the entire cycle was elucidated which involves a hispidin-synthase (HispS), a hispidin 3-hydroxylase (H3H), a luciferase (Luz), and a caffeylpyruvate hydrolase (CPH). The cluster encompassing the respective genes was found to be conserved in other luminescent fungi. This suggests that all luminescent fungi share the same luciferin/luciferase system. The enzymes and

Downloaded from http://www.jbc.org/ at University of Groningen on September 15, 2020

chemistry involved do not show any resemblance with other hitherto known bioluminescence systems (Scheme 1). Recently, a plant was equipped with the fungal genes responsible for luminescence. Upon insertion of the four mentioned genes from the bioluminescent mushroom *Neonothopanus nambi* into the DNA of tobacco plants, luminous plants were created (17). The functioning of the fungal system in tobacco plants confirms that it can simply be fueled with the plant endogenous substrate caffeic acid. The luminescence was also found to be superior when compared with the bacterial luminescence system, demonstrating that the fungal light-emitting enzyme system has attractive features.

Here, we report on the heterologous recombinant expression, purification and biochemical characterization of hispidin 3-hydroxylase from *Mycena chlorophos* (McH3H) (18). This enzyme was found to be a monomeric NAD(P)H-dependent, FAD-containing monooxygenase, which catalyzes the hydroxylation of hispidin to form 3-hydroxyhispidin (Scheme 1). The study provides the first detailed insights into the properties of a fungal luciferin-producing enzyme and has resulted in enzyme variants with different nicotinamide cofactor specificities. The developed expression system and elucidated catalytic features provide a good basis for further studies into the molecular mechanisms of fungal bioluminescence.

## Results

### Expression and purification

While the genes responsible for luminescence in the prototype light-emitting fungus *M. chlorophos* have been identified, the respective enzymes have not been studied in detail. To investigate the enzymatic properties of a fungal luciferin-producing hydroxylase, we decided to express the putative hispidin hydroxylase from *M. chlorophos*: McH3H. A BLAST search (NCBI) with the McH3H protein sequence confirmed that this enzyme is a representative of many homologous fungal proteins that appear to be orthologs in view of the relatively high sequence identity. A search in the database of proteins for which the three-dimensional structure has been elucidated, confirmed sequence relationship with well-studied class A flavoprotein monooxygenases (19, 20). These monooxygenases are single component monooxygenases, that typically contain a tightly bound FAD cofactor and depend on NADPH and/or NADH as coenzyme for activity. The highest sequence identity (29 %) was found with salicylate hydroxylase from *Pseudomonas putida* G7 (PpSALH) (21). A multiple sequence alignment of McH3H, PpSALH, 3-hydroxybenzoate 6-hydroxylase from *Rhodococcus jostii* RHA1 (Rj3HB6H) and *p*-hydroxybenzoate hydroxylase from *Pseudomonas fluorescens* (PfPHBH, the prototype class A flavoprotein monooxygenase) revealed conservation of several canonical sequence motifs (GxGxxG, GD and DG motifs) (Fig. S1). At the N-terminus, a GxGxxG sequence motif is conserved which forms part of the Rossmann fold domain that binds the ADP moiety of the FAD cofactor (Fig. S1) (22). The sequence of McH3H also contains other conserved regions that confirm a similar binding mode of the FAD cofactor (23). Furthermore, the sequence differs significantly from PfPHBH in the region encompassing residues 40-50. The corresponding part in the structure of PfPHBH has been shown to tune the coenzyme specificity towards NADPH (24) and may suggest that McH3H has a different coenzyme specificity (25).

McH3H was produced as His-tagged SUMO fusion protein in *E. coli* NEB10β cells. About 100 mg SUMO-McH3H per liter of culture could be purified using immobilized metal affinity chromatography. Based on the amino acid sequence the theoretical molecular mass of His-tagged SUMO-McH3H is 60 kDa and that of McH3H is 46 kDa. According to SDS-PAGE analysis, the purification indeed resulted in a protein with the predicted mass of the fusion protein (65 kDa) (Fig. S2A). Upon removal of the His-tagged SUMO, untagged McH3H was obtained. Gel permeation experiments with the cleaved McH3H revealed an apparent molecular mass of about 43 kDa (Fig. S2B), indicating that in solution, the enzyme is monomeric. The purified protein had an intense yellow color which is in line with the observation that its sequence contains all hallmark sequence motifs of a class A flavoprotein monooxygenase that typically harbors a tightly bound FAD cofactor. The UV-Vis absorption spectrum of McH3H

Downloaded from http://www.jbc.org/ at University of Groningen on September 15, 2020

revealed typical flavoprotein features, with absorption maxima at 375 nm and 450 nm (Fig. S3). The A280/A450 was 5.5 and confirms that the enzyme is predominantly in the holo form as the theoretical A280/A450 ratio calculated by using the calculated extinction coefficient at 280 nm and the determined extinction coefficient at 450 nm is 4.8. Treatment with 0.2% SDS resulted in a slightly altered spectrum due to release of the flavin cofactor (Fig. 1). The identity of the cofactor as FAD was confirmed upon treatment with phosphodiesterase which resulted in formation of FMN. Since chloride and other monovalent anions are inhibitors of several class A enzymes, such as PfPHBH, 3HB6H and PpSALH, chloride and phosphate ions were tested. Yet, no significant effect on the activity (< 10%) of McH3H was observed in the presence of 100 mM chloride or phosphate.

**Catalytic properties and steady-state kinetics**

Before testing activity of McH3H with hispidin, suitable experimental conditions were established. It was found that hispidin absorbs in the visible region and that the UV-Vis absorption spectrum of hispidin is highly influenced by pH. This complicates the use of the commonly used assay in which the consumption of NAD(P)H is monitored by measuring the absorbance decrease at 340 nm over time. On top of that, we observed that hispidin seems to decay in certain buffers. Based on the performed tests (several buffer types and pH values), we concluded that potassium phosphate is the most suitable buffer to use as it showed minimal effects on the absorption spectrum of hispidin at different pH values. Hence, all biochemical studies of McH3H were carried out using potassium phosphate buffer. The wavelength for the absorption maximum of hispidin changes with pH (Fig. S4). This is because hispidin contains several hydroxy groups with relatively low p*K*a values. To avoid pH-induced artefacts on activity measurements, we opted for assaying the enzyme activity by using a dioxygen sensing device, as McH3H uses molecular oxygen for the hydroxylation of hispidin (Scheme 1).

Gratifyingly, we could indeed confirm that McH3H is active on hispidin. Using 100 μM NADPH, 40 μM hispidin and 25 nM McH3H, a rapid consumption of dioxygen was observed. Under the experimental conditions applied, the enzyme shows a rather broad pH optimum, with the highest activity between pH 7.0 and 8.0 (Fig. 2A). The thermal stability of the enzyme at different pH values was analyzed by measuring the apparent melting temperature ($T_m$) using the ThermoFAD method (26) (Fig. 2B). This revealed that McH3H is most stable at pH 7.0 with an apparent $T_m$ of 42 °C. Based on these results we decided to use 50 mM potassium phosphate, pH 7.0 as standard buffer for all subsequent experiments. The ThermoFAD method was also used to study the effect of substrate binding on the melting temperature of the enzyme. Interestingly, the $T_m$ was greatly impacted by hispidin: it went from 42 ˚C in the absence of hispidin up to 50 ˚C with apparent saturating hispidin concentrations. This analysis also allowed determination of the apparent dissociation constant ($K_d$) of hispidin: 45 μM (Fig. S5).

For definite proof for the role of McH3H in 3-hydroxyhispidin production, we set out to determine the formed product. The recombinant enzyme was used to transform 1.0 mg hispidin after which the reaction product was isolated and characterized by $^1$H NMR. It was found that McH3H can indeed catalyze the full transformation of hispidin into 3-hydroxyhispidin (Fig. 3). No other oxidized products were detected. A range of other compounds (including 4-hydroxy-*2H*-pyrone, 4-methoxy-6-methyl-*2H*-pyran-one, *2H*-pyran-2-one and various phenols) were also tested as possible substrates (Fig. S6). However, HPLC or GC analysis showed that none of the tested compounds showed any conversion. This suggests that McH3H is extremely specific for hispidin. A narrow substrate acceptance profile is fairly common for class A flavoprotein hydroxylases.

To further confirm that the product (3-hydroxyhispidin) formed by action of McH3H is the substrate for the fungal luciferase (McLuz) catalyzed light production, a luminescence reaction experiment was carried out. This revealed that visible (green) light can be observed in a dark environment upon mixing McH3H, NADPH, hispidin and *E. coli* cells expressing McLuz (Fig. S7). Omission of any of the components abolished light production. This convincingly shows that McH3H is a true luciferin-producing enzyme.

Downloaded from http://www.jbc.org/ at University of Groningen on September 15, 2020

Interestingly, except for identifying hispidin as substrate, McH3H was found to show activity with NADH or NADPH as coenzyme. This is somewhat rare for class A flavoprotein monooxygenases; they are usually rather specific for one nicotinamide coenzyme. To establish whether there was a preference for one of the coenzymes, we carried out steady-state kinetics experiments. The steady-state kinetic parameters were determined at 25°C. While McH3H displayed similar apparent $k_{cat}$ values for NADPH (6.0 $s^{-1}$) and NADH (6.7 $s^{-1}$) in the presence of 50 µM hispidin (Fig. 4A and 4B), the $K_M$ value for NADPH was significantly lower than for NADH (69 µM vs. 240 µM). The apparent $K_M$ of the enzyme for hispidin was found to be rather low with a $K_M$ of around 5 µM (Fig. 4C and 4D), independent of the used coenzyme. In the absence of hispidin, McH3H also consumed dioxygen and, hence, acted as a slow NAD(P)H oxidase. At 500 µM NADPH or NADH, this activity was 0.2 $s^{-1}$ and 0.1 $s^{-1}$, respectively. These results show that hispidin, besides being a substrate, also acts as an effector, strongly stimulating coenzyme consumption. Class A flavoprotein monooxygenases are known to display uncoupling: consumption of the reduced coenzyme which does not lead to hydroxylation, resulting in hydrogen peroxide formation (27). The McH3H uncoupling rate was determined by measuring the hydrogen peroxide formation and revealed 30% uncoupling when NADPH was used and 15% uncoupling in the case of NADH.

**Rapid kinetics**

After determining the steady-state kinetics of McH3H, we performed a rapid kinetics analysis of McH3H to elucidate its kinetic mechanism. The reaction cycle of most flavoenzymes typically follows two phases, a reductive half-reaction and an oxidative half-reaction (28–30).

First, the reductive half-reaction was studied by conducting reactions in the absence of dioxygen. Since McH3H shows a preference for NADPH over NADH, the respective rapid kinetics experiments were carried out using NADPH. The dissociation constants of the binary McH3H·NADPH complex and of the ternary McH3H·NADPH·hispidin complex were determined by measuring the reduction rate of the protein at different NADPH concentrations and monitoring the reaction at 450 nm. The reduction rate of the enzyme, while proceeding extremely slow without hispidin, is strongly boosted when hispidin is present (with reduction rates going from 2.7 $s^{-1}$ to 220 $s^{-1}$) (Fig. 5A and 5B). Clearly, binding of substrate triggers efficient reduction of the flavin cofactor by NADPH. The dissociation constants ($K_d$) of NADPH for the McH3H·NADPH complex and McH3H·NADPH·hispidin complex were 2.8 mM and 0.8 mM, respectively (Fig. 5A and 5B). Subsequently, the affinity for hispidin was determined by varying the hispidin concentration while maintaining a fixed concentration of NADPH (Fig. 5C). This corroborated the above findings that the hydroxylase has a high affinity towards its aromatic substrate ($K_{d,hispidin}$ = 4.1 µM). The redox state of the flavin cofactor was also monitored under aerobic conditions upon mixing the enzyme with only NADPH or with NADPH and hispidin (Fig. 5D). This showed that the enzyme remains mainly in the oxidized state when only NADPH is available. This fully agrees with the slow rate of flavin reduction in the absence of hispidin. When hispidin is present, a fast and significant reduction of the flavin absorbance is observed, reaching an equilibrium after 0.1 s. This suggests that during steady-state kinetics, the rate of reduction is not rate-limiting. This is also expected considering the relatively fast rate of FAD reduction (>200 $s^{-1}$).

The second half of the reaction cycle was studied by mixing the anaerobically reduced enzyme with oxygenated buffer. To follow the oxidative half-reaction, we initially monitored the spectral changes occurring after mixing the fully NADPH-reduced McH3H with aerobic buffer in the absence and presence of substrate. In the absence of substrate, reduced McH3H reacted rapidly with dioxygen, without observing a C4a-hydroperoxyflavin intermediate formation. The intermediate typically has an absorbance maximum at 360-390 nm (Fig. 6A). The reaction led to full reoxidation of the FAD cofactor in an apparent single kinetic event. When using 10 µM hispidin in the oxidative half-reaction, a similar fast and full reoxidation was observed (Fig. 6B). The kinetic and spectral changes between these two experiments were minimal indicating that, even in the presence of hispidin, McH3H is not efficient in stabilizing the

Downloaded from http://www.jbc.org/ at University of Groningen on September 15, 2020

oxygenating flavin intermediate. Low temperature condition (4°C) and the addition of sodium azide did not help to stabilize the hydroperoxyflavin. This observation is in line with the observed poor coupling efficiency, *vide supra*. Yet, lack of stabilization of the presumed C4a-(hydro)peroxyflavin species is not an uncommon phenomenon for class A flavoprotein monooxygenases. The dioxygen concentration dependency of the reoxidation kinetics displayed saturating behavior (see insets Fig. 6). This is somewhat unusual for class A flavoprotein monooxygenases but has been observed in some flavoenzymes (31, 32) and suggests a binding event of molecular oxygen before it reacts with the reduced flavin.

**Pyridine nucleotide coenzyme specificity of McH3H**

The preference of McH3H for NADPH was somewhat unanticipated as it shows relatively high sequence identity with other flavoprotein hydroxylases displaying high specificity for NADH. In absence of a crystal structure (crystallization trials of McH3H failed), we generated a homology model using YASARA (33) and performed a structural alignment with the strict NADPH-dependent PfPHBH (PDB entry 1PBE). Guided by the structural comparison of our model with the PfPHBH structure and by the work from Eppink et al. (1999), we designed mutants in a loop which in McH3H ranges from residue 40 to 48. While the loop in our model assumes a relaxed conformation, because of the absence of the FAD cofactor in the modeled structure, its role can be clearly deduced from the topological equivalent region in PfPHBH (residues 32 to 43) (Fig. S8). Based on this comparison and on previous studies on PfPHBH, we identified residues Phe44, Lys45 and Thr46 as candidates for mutagenesis. Upon further comparative analysis of our model with the structure of a flavoprotein hydroxylase from *Pseudomonas aeruginosa* (PDB entry 3C96), we decided to generate point mutations at these positions, introducing glutamate residues. Gratifyingly, all three mutants displayed significantly reduced $K_M$ values for NADH while the $K_M$ values for NADPH increased and the $k_{cat}$ values were not or only mildly affected (Table 1). The most striking mutant was McH3H-F44E which is much more efficient with NADH. This variant shows a 11-fold reduction of the $K_M$ for NADH (22 μM), while the $K_M$ for NADPH is also affected by one order of magnitude in the opposite direction (810 μM). As a result, this mutant McH3H displays an opposite cofactor preference when compared with the wild-type enzyme. Interestingly, the T46E mutation resulted in a variant which is essentially indifferent towards the two nicotinamide cofactors (Table 1). Clearly, the cofactor specificity depends on subtle interactions and can be easily altered by single mutations. The created NADH-specific McH3H may be of interest when considering the hydroxylase as biocatalyst due to the low costs of NADH when compared with NADPH.

**Discussion**

In the present study, we demonstrate that hispidin 3-hydroxylase from *M. chlorophos* can be well expressed in *E. coli* as a soluble monomeric FAD-containing protein. The enzyme could be purified by affinity chromatography and its properties were studied. Chemical analysis confirmed that McH3H performs a regioselective *ortho*-hydroxylation of hispidin to generate 3-hydroxyhispidin as single aromatic product. No other aromatic substrates for McH3H could be identified, suggesting that the hydroxylase is highly substrate specific. The strict substrate specificity of McH3H may be related to its specific role in hispidin-based luciferin biosynthesis in fungi as part of the fungal bioluminescence process (16).

McH3H accepts both pyridine nucleotide cofactors, NADH and NADPH, with a preference for NADPH. These characteristics are in line with common features of class A flavoprotein monooxygenases. In fact, McH3H shares significant sequence similarity with PfPHBH, a well-studied NADPH-dependent FAD-containing hydroxylase (34, 35). Both enzymes also display similar reductive half-reaction kinetic characteristics: substrate binding triggers a fast NADPH-mediated reduction of the FAD cofactor. In the absence of hispidin, McH3H shows a very low but significant NAD(P)H oxidase activity. In the oxidative half-reaction, not all formed peroxyflavin is used for hydroxylation as significant uncoupling is observed. In fact, stopped-flow experiments indicate that the enzyme does not stabilize the peroxyflavin intermediate, as observed with other class A flavoprotein monooxygenases.

Downloaded from http://www.jbc.org/ at University of Groningen on September 15, 2020

Nevertheless, the oxygen consumption experiments show that most of the consumption of NADPH is coupled to a highly regioselective hydroxylation of hispidin.

A sequence comparison study revealed that the hispidin-3-hydroxylases in luminescent fungi display high sequence identities in the pyridine nucleotide coenzyme specificity loop (residues from 40 to 50 in McH3H). This high sequence conservation (Fig S9A), indicates that H3H in luminescent fungi may have a similar coenzyme preference for NADPH. However, McH3H also shows sequence similarity to hydroxylases with different coenzyme preferences, such as PfPHBH (NADPH >> NADH), RoPHBH (NADH >> NADPH), PpSALH and Rj3HB6H (NADH > NADPH) (36–39). Amino acid sequence alignment analysis shows that the pyridine nucleotide coenzyme recognition region among these enzymes is less conserved (Fig S9B). Based on this, several mutants of McH3H were prepared which revealed that the coenzyme specificity of McH3H could be tuned. The obtained results are in accordance with the more general finding that the adenosine 2'-phosphate of NADPH prefers to interact with positively charged residues whereas the 2'OH of NADH prefers to interact with negatively charged residues (40) Similar findings with other flavoprotein monooxygenases have been reported (41, 42). McH3H mutants with opposite coenzyme specificity (NADH preference) or an indifference towards nicotinamide coenzymes were created. Such variants of McH3H may develop as valuable biocatalysts for use of the hydroxylase in developing novel bioluminescence tools. Except for optimal intracellular exploitation of the available coenzymes, tuned mutants may even be used for probing the presence of coenzyme levels.

In the present work, we experimentally demonstrate that McH3H is a soluble monomeric NAD(P)H-dependent, FAD-containing hydroxylase that catalyzes the hydroxylation of hispidin to form 3-hydroxyhispidin. Rapid kinetic analysis revealed that McH3H has a high affinity for hispidin. The kinetic data demonstrate that formation of the ternary complex, McH3H·NADPH·hispidin, accelerates the reduction process of FAD by NADPH to initiate hydroxylation of hispidin. Thus, reduction of McH3H is triggered by binding of hispidin, speeding up the overall reaction rate, and limiting uncoupling when no hispidin is present. Residues have been identified that tune the coenzyme specificity. This resulted in mutants with a preference for NADH as electron donor. The ability to use NADH is an attractive feature for the usage of the enzyme as a biocatalyst as NADPH is relatively costly. Furthermore, enzyme variants optimized for the use of both cofactors may boost the performance of fungal luminescent systems in recombinant organisms, such as engineered luminescent plants (17).

## Materials and methods

### Chemicals, reagents, and strains

NADPH and $NADP^+$ were purchased from Oriental Yeast Co. LTD. NADH was purchased from Roche Diagnostics. Ni Sepharose™ 6 fast flow was purchased from GE Healthcare. T4 ligase and the restriction enzyme BsaI were purchased from New England Biolabs. *E. coli* NEB10 β (New England Biolabs) strain was used as host for cloning and protein expression. All other chemicals were ordered from Sigma-Aldrich. Hispidin was chemically synthesized using a previously published protocol (43).

### Plasmid construction and transformation

The *E. coli* codon-optimized *h3h* gene (GenBank: BBH43493.1) and *luz* gene (GenBank: LC435377.1) from *M. chlorophos* were synthesized by Integrated DNA Technologies. The *mch3h* and *mcluz* genes were cloned into pBAD-His6x-SUMO and pET-28b (+)-His6x-SUMO (Small Ubiquitin-like Modifier) vectors, respectively, by using the Golden Gate cloning approach. These two vectors contained two BsaI restriction sites, with an upstream region coding for an N-terminal His6 tag. This pBAD-His6x-SUMO vector has an araC promoter, and an ampicillin resistance gene. The pET-28b (+)-His6x-SUMO vector has a lcaI promoter, and a kanamycin resistance gene. The Golden Gate reaction mixture contained Golden Gate pBAD-His6x-SUMO or pET-28b (+)-His6x-SUMO vectors, BsaI restriction enzyme, T4 ligase, ligation buffer, *h3h* or *luz* gene, and sterile Milli-Q water. The incubation temperature alternated

Downloaded from http://www.jbc.org/ at University of Groningen on September 15, 2020

between 37 °C for 5 min and 16 °C for 10 min for 30 cycles, then was then set to 55°C for 10 min, and finally to 65°C for 20 min to inactivate the enzymes. 4 µl of the reaction mixture was added to chemically competent *E. coli* NEB 10β cells to do the transformation. After overnight growth on an LB agar plate with ampicillin, colonies were picked and grown in LB medium with ampicillin. The plasmids were isolated and sent for sequencing (GATC, Germany) to confirm the correct ligation of the genes.

**Enzyme production, purification, and storage**

The recombinant strain *E. coli* NEB10 β, carrying the *h3h* gene, was incubated at 24 ºC for 24 h in 200 ml TB medium containing 50 µg/ml ampicillin. L-arabinose was added (0.02% w/v) when $OD_{600}$ was around 1.0. Cells were harvested at 4 °C and centrifuged at 6000 rpm using the JLA10.500 rotor for 20 min in the Beckman-Coulter centrifuge. Cells were then resuspended in 50 mM potassium phosphate buffer at pH 7.5, containing 0.25 M KCl, 1 µg/ml DNase, and 0.1 mM phenylmethylsulfonyl fluoride. Resuspended cells were disrupted by sonication and centrifuged at 4 °C at 12,000 rpm using the JA17 rotor for 1 hour. The 2 ml HisTrap Ni-Sepharose HP column (GE Healthcare Lifesciences, USA) was first equilibrated using 50 mM potassium phosphate buffer pH 7.5. Then the cell-free extract was loaded to the column. 50 mM potassium phosphate buffer pH 7.5 was used to wash off non-specifically bound proteins from the column. 50 mM potassium phosphate buffer pH 7.5 with 10 mM imidazole was then used to wash off weakly bound proteins. The enzymes then eluted using 50 mM potassium phosphate buffer pH 7.5 with 100 mM imidazole. The eluted fraction containing McH3H were desalted by using the HiPrep 26/10 Desalting column (GE Healthcare Lifesciences) using 50 mM potassium phosphate buffer pH 7.5. Enzymes aliquots were frozen using liquid nitrogen and stored at -80 °C until further use. The concentration of purified McH3H was determined by using a molar absorption coefficient of 11,000 $M^{-1}$ $cm^{-1}$ at 450 nm (FAD)**.** The molar absorption coefficient was determined by 0.2% SDS treatment of an enzyme sample and comparison with the known FAD absorption spectrum (44). To establish the identity of the McH3H-bound flavin cofactor, phosphodiesterase (PDE) treatment was used that involves hydrolysis of FAD into FMN, as described previously (44). The theoretical molecular mass of McH3H was calculated based on the amino acid sequence by using the Compute pI/Mw tool at ExPASy Proteomics Server (https://www.expasy.org/) (45, 46). To produce McLuz protein, the plasmid, pET-28b (+)-His6x-SUMO-McLuz, was transformed into *E. coli* strain BL21 (DE3) cells. Proteins were expressed in TB medium containing 50 µg/ml kanamycin by induction of 0.4 mM IPTG at 24 °C for 24 h. Cells were harvested at 4 °C and centrifuged at 6000 rpm using the JLA10.500 rotor for 20 min in the Beckman-Coulter centrifuge. The pellet was washed by using 50 mM potassium phosphate buffer at pH 7.5, and then saved at -20 ºC.

**Product characterization by NMR analysis**

To identify the aromatic reaction product of McH3H by NMR analysis (Bruker Avance NEO 600 - 600 MHz), a semi-preparative conversion of hispidin was performed. The reaction mixture contained 1.0 mg hispidin, 10 µM McH3H, 10 µM PTDH, 200 µM $NADP^+$, 10 mM sodium phosphite, 100 mg DTT in 50 mM potassium phosphate buffer, pH 7.5 (final reaction volume was 5 ml). The reaction was performed in a closed 20 ml glass vial at 30 °C for 20 min. After that, the reaction was quenched by adding 150 µl of concentrated hydrochloric acid, and the product was extracted with ethyl acetate (3 x 5 ml). The extract was dried under anhydrous $MgSO_4$, filtered, and concentrated under reduced pressure. The crude product was analyzed without further purifications by NMR. The control reaction was performed under the same reaction conditions without 10 µM McH3H.

**Substrate specificity analyzed by HPLC and GC-MS**

Reaction mixtures (1 ml) used for HPLC analysis on AS-2050 Plus (JASCO, Japan) contained 5.0 mM test compound, 20 µM McH3H, 20 µM PTDH, 200 µM $NADP^+$, 10 mM sodium phosphite, in 50 mM potassium phosphate buffer, pH 8.0. The reaction was performed in a closed 4 ml glass vial at 25°C for 24 hours. After that, a 20 µl sample was mixed with 80 µL acetonitrile and the samples were centrifuged at high speed for 5 minutes. The supernatant was analyzed by using Zorbax Eclipse

Downloaded from http://www.jbc.org/ at University of Groningen on September 15, 2020

XDB-C8 column (5 µm, Agilent). The control reaction was performed under the same reaction conditions without McH3H.

Reaction mixtures (1 ml) used for GC-MS analysis on GCMS-QP2010 (SHIMADZU, Japan) contained 1.0 mM test compound, 5 µM McH3H, 10 µM PTDH, 100 µM $NADP^+$, 10 mM sodium phosphite, in 50 mM potassium phosphate buffer, pH 8.0. The reaction was performed in a closed 4 mL glass vial at 25 ℃ for 24 hours. After that, a 500 µL sample was taken for extraction with ethyl acetate (1 x 250 µl). The extracted product was dried under anhydrous $MgSO_4$ and analyzed by using HP-1MS column (30 m x 0.25 mm x 0.25 µm, Agilent). control reaction was performed under the same reaction conditions without McH3H.

**pH optimum**

The activity of the enzyme was evaluated at different pH values by monitoring oxygen consumption at 25 ºC using purified protein (25 nM) in a 50 mM potassium phosphate buffer containing 100 µM NADPH and 20 µM hispidin. The reaction (total volume 1 ml) was initiated by adding the enzyme. Oxygen consumption was measured on an Oxygraph plus system (Hansatech Instruments Ltd, England). Initial rates were determined from the initial linear parts of the reaction curves.

**Thermal stability assays**

To determine the pH effect on the thermostability of McH3H, the enzyme was evaluated at different pH values by measuring the apparent melting temperature using the ThermoFAD method (26). The incubations (20 µl) contained 10 µM purified protein in 50 mM potassium phosphate buffer at varying pH. Using an RT-PCR thermocycler, intensity of flavin fluorescence was measured while the samples were heated up from 25 to 90 ℃ with 0.5 ℃ per step, using a holding time of 10 s at each step. The maximum of the first derivative of the observed flavin fluorescence was taken as the apparent melting temperature.

**McH3H uncoupling rate determination**

McH3H uncoupling rate was determined by following the hydrogen peroxide formation. This experiment was carried out in 1 mL reaction mixture containing 500 µM hispidin and 1 mM NADPH or NADH, and the reaction was initiated by adding 0.3 µM McH3H. Enough catalase (1000 U) was then added to the 1 ml reaction when the reaction rate was still in the linear phase. The addition of catalase instantly caused an increase in oxygen concentration, as hydrogen peroxide could produce water and dioxygen. The reactions were performed in 50 mM potassium phosphate buffer (pH 7.0) at 25ºC by using an Oxygraph plus system (Hansatech Instruments Ltd, England). The relative activities were calculated as follows:

$$Uncoupling\ rate = (2\ \mathrm{A})/\mathrm{B} \qquad (1)$$

Where A is the oxygen concentration increased after adding catalase, B is total oxygen consumed in the reaction.

**Steady-state kinetics**

The kinetics parameters of McH3H toward hispidin, and NAD(P)H were determined in 50 mM potassium phosphate buffer (pH 7.0) at 25 ºC by monitoring oxygen consumption. Stock solutions of hispidin were prepared in methanol. The final concentration of methanol in the test reaction was kept below 5% (v/v). The reaction mixture kept 1 ml and the reaction was initiated by adding the enzyme. Oxygen consumption was measured on an Oxygraph plus system (Hansatech Instruments Ltd, England). Initial rates were determined from the initial linear parts of the reaction curves by varying the concentration of the substrate (or coenzyme) at a fixed concentration of the coenzyme (or substrate). Kinetics data were fitted with the Michaelis-Menten equation using the Graphpad Prism (version 6.07) to obtain the steady-state kinetic parameters.

**Rapid kinetics**

The reductive and oxidative half-reactions of McH3H were studied using the single-mixing mode of a SX20 stopped-flow spectrophotometer equipped with a photodiode array detector (Applied Photophysics, Surrey, UK). All solutions were prepared in 50 mM potassium phosphate pH 7.0 buffer. Reactions were run in technical duplicate by

Downloaded from http://www.jbc.org/ at University of Groningen on September 15, 2020

mixing equal volumes of two solutions at 25 °C. The set-up conditions of reductive and oxidative half-reactions were prepared following the general methods previously described (47). The stopped-flow traces at 375 nm and 450 nm were fitted to exponential functions to determine the observed rates ($k_{obs}$). All data were analyzed using the software Pro-Data (Applied Photophysics, Surrey, UK) and GraphPad Prism 6.07 (La Jolla, CA, USA).

**Gel permeation analysis**

SUMO was cleaved from the McH3H by adding SUMO protease, then McH3H without SUMO was used for gel filtration analysis on AKTA purifier (GE Healthcare Lifesciences, USA). The recombinant enzyme solution McH3H without SUMO (10 mg/ml) was applied to a (GE Healthcare Lifesciences, USA) equilibrated with 50 mM Tris-HCl (pH 7.5) buffer containing 200 mM NaCl. Bovine serum albumin ($M_r$ 67,000 Da), ovalbumin ($M_r$ 43,000 Da), ribonuclease A ($M_r$ 13,700 Da), aprotinin ($M_r$ 6,512 Da), and vitamin B12 (1,350 Da) were used as reference proteins for the estimation of the apparent molecular mass.

**Homology modeling and mutants design**

The amino acid sequence of McH3H was used to run homology modeling on YASARA following the standard procedure offered by the program. A model was generated based on the PDB entry 6BZ5 of salicylate hydrolase (21). Upon inspection of the model, superposition with the crystal structure of PfPHBH (PDB entry 1PBE) and PaFMO (PDB entry 3C96), and sequence alignment, the residue Glu39 present in PaFMO was introduced in the McH3H sequence in positions 44, 45 or 46, generating different variants of the wild type enzyme.

**Site-directed mutagenesis**

The site-directed mutagenesis was carried out by using the pBAD-SUMO-McH3H vector as a template. The primers used are listed in Table 2 and the PCR processes are the following. The 20 µl PCR reaction mixture contained 30 ng template, 0.2 µM (each) mixed primers and 10 µl PfuUltra II Hotstart PCR Master Mix, which contained optimized PCR reaction buffer, magnesium, and dNTPs. The 20 µl mixture was subjected to the following PCR conditions: 95 °C for 2 min, 30 cycles of 95 °C for 20 s, 55 °C for 30 s and 72 °C for 2 min, and a final extension at 72 °C for 10 min. The PCR products were digested with DpnI at 37 °C to remove the parental templates, after which the reaction mixtures were transformed into chemically competent *E. coli* NEB 10 β.

**Data availability**

All data are contained within the manuscript.

Downloaded from http://www.jbc.org/ at University of Groningen on September 15, 2020

**Acknowledgment**

Y. Tong thanks the China Scholarship Council for a Ph.D. fellowship.

**Author Contributions**

Y. Tong performed the experiments and drafted the manuscript. M. Trajkovic synthesized the compounds needed for the experiment and carried out the NMR experiments. S. Savino designed mutants for the coenzyme specificity. W.J.H. van Berkel and M.W. Fraaije participated in data analysis and manuscript preparation. The manuscript received contribution from all authors.

**Conflicts of Interest**

Authors declare no conflict of interests regarding the contents of this manuscript.

## References


1. Harvey E. Newton (1957) Shining Fish, Flesh, and Wood. in A history of luminescence from the earliest times until 1900, pp. 461–507, *Philadelphia,American Philosophical Society*, https://doi.org/10.5962/bhl.title.14249
2. Chew, A. L. C., Tan, Y. S., Desjardin, D. E., Musa, M. Y., and Sabaratnam, V. (2014) Four new bioluminescent taxa of Mycena sect. Calodontes from Peninsular Malaysia. *Mycologia*. **106**, 976–988
3. Desjardin, D. E., Oliveira, A. G., and Stevani, C. V. (2008) Fungi bioluminescence revisited. *Photochemical and Photobiological Sciences*. **7**, 170–182
4. Oliveira, A. G., Desjardin, D. E., Perry, B. A., and Stevani, C. V. (2012) Evidence that a single bioluminescent system is shared by all known bioluminescent fungal lineages. *Photochemical and Photobiological Sciences*. **11**, 848–852
5. Stevani, C. V., Oliveira, A. G., Mendes, L. F., Ventura, F. F., Waldenmaier, H. E., Carvalho, R. P., and Pereira, T. A. (2013) Current status of research on fungal bioluminescence: biochemistry and prospects for ecotoxicological application. *Photochemistry and Photobiology*. **89**, 1318–1326
6. Airth R. L. & Mceloy W. D. (1958) Light emission from extracts of luminous fungi. *Journal of bacteriology*. **77**, 249–250
7. Airth R.L. & Foerster G.E (1962) The isolation of catalytic components required for cell-free fungal bioluminescence. *Archives of Biochemistry and Biophysics*. **97**, 567–573
8. Airth R. L. & Foerster G. E (1964) Enzymes associated with bioluminescence in *Panus Stypticus* luminescens and *Panus Stypticus* non-luminescens. *Journal of bacteriology*. **88**, 1372–1379
9. Mori, K., Kojima, S., Maki, S., Hirano, T., and Niwa, H. (2011) Bioluminescence characteristics of the fruiting body of *Mycena chlorophos*. *Luminescence*. **26**, 604–610
10. Teranishi, K. (2016) Localization of the bioluminescence system in the pileus of *Mycena chlorophos*. *Luminescence*. **31**, 594–599
11. Teranishi, K. (2016) Trans-*p*-hydroxycinnamic acid as a bioluminescence-activating component in the pileus of the luminous fungus *Mycena chlorophos*. *Tetrahedron*. **72**, 726–733
12. Teranishi, K. (2017) Second bioluminescence-activating component in the luminous fungus *Mycena chlorophos*. *Luminescence*. **32**, 182–189
13. Teranishi, K. (2016) Identification of possible light emitters in the gills of a bioluminescent fungus *Mycena chlorophos*. *Luminescence*. **31**, 1407–1413
14. Purtov, K. V., Petushkov, V. N., Baranov, M. S., Mineev, K. S., Rodionova, N. S., Kaskova, Z. M., Tsarkova, A. S., Petunin, A. I., Bondar, V. S., Rodicheva, E. K., Medvedeva, S. E., Oba, Y., Oba, Y., Arseniev, A. S., Lukyanov, S., Gitelson, J. I., and Yampolsky, I. V. (2015) The chemical basis of fungal bioluminescence. *Angewandte Chemie - International Edition*. **54**, 8124–8128
15. Kaskova, Z. M., Dörr, F. A., Petushkov, V. N., Purtov, K. V., Tsarkova, A. S., Rodionova, N. S., Mineev, K. S., Guglya, E. B., Kotlobay, A., Baleeva, N. S., Baranov, M. S., Arseniev, A. S., Gitelson, J. I., Lukyanov, S., Suzuki, Y., Kanie, S., Pinto, E., Mascio, P. Di, Waldenmaier, H. E., Pereira, T. A., Carvalho, R. P., Oliveira, A. G., Oba, Y., Bastos, E. L., V. Stevani, C., and Yampolsky, I. V. (2017) Mechanism and color modulation of fungal bioluminescence. *Science Advances*. **3**, e1602847
16. Kotlobay, A. A., Sarkisyan, K. S., Mokrushina, Y. A., Marcet-Houben, M., Serebrovskaya, E. O., Markina, N. M., Somermeyer, L. G., Gorokhovatsky, A. Y., Vvedensky, A., Purtov, K. V., Petushkov, V. N., Rodionova, N. S., Chepurnyh, T. V., Fakhranurova, L. I., Guglya, E. B., Ziganshin, R., Tsarkova, A. S., Kaskova, Z. M., Shender, V., Abakumov, M., Abakumova, T. O., Povolotskaya, I. S., Eroshkin, F. M., Zaraisky, A. G., Mishin, A. S., Dolgov, S. V., Mitiouchkina, T. Y., Kopantzev, E. P., Waldenmaier, H. E., Oliveira, A. G., Oba, Y., Barsova, E., Bogdanova, E. A., Gabaldón, T., Stevani, C. V., Lukyanov, S., Smirnov, I. V., Gitelson, J. I., Kondrashov, F. A., and Yampolsky, I. V. (2018) Genetically encodable bioluminescent system from fungi. *Proceedings of the National Academy of Sciences of the United States of America*. **115**, 12728–


Downloaded from http://www.jbc.org/ at University of Groningen on September 15, 2020

12732
17. Mitiouchkina, T., Mishin, A. S., Somermeyer, L. G., Markina, N. M., Chepurnyh, T. V, Guglya, E. B., Karataeva, T. A., Palkina, K. A., Shakhova, E. S., Fakhranurova, L. I., Chekova, S. V, Tsarkova, A. S., Golubev, Y. V, Negrebetsky, V. V, Dolgushin, S. A., Shalaev, P. V, Shlykov, D., Melnik, O. A., Shipunova, V. O., Deyev, S. M., Bubyrev, A. I., Pushin, A. S., Choob, V. V, Dolgov, S. V, Kondrashov, F. A., Yampolsky, I. V, and Sarkisyan, K. S. (2020) Plants with genetically encoded autoluminescence. *Nature Biotechnology*. 10.1038/s41587-020-0500-9
18. Sato, T., Uzuhashi, S., Hosoya, T., and Hosaka, K. (2010) A list of fungi found in the bonin (Ogasawara) islands. *biology*. **35**, 59–160
19. van Berkel, W. J. H., Kamerbeek, N. M., and Fraaije, M. W. (2006) Flavoprotein monooxygenases, a diverse class of oxidative biocatalysts. *Journal of Biotechnology*. **124**, 670–689
20. Huijbers, M. M. E., Montersino, S., Westphal, A. H., Tischler, D., and van Berkel, W. J. H. (2014) Flavin dependent monooxygenases. *Archives of Biochemistry and Biophysics*. **544**, 2–17
21. Costa, D. M. A., Gómez, S. V., de Araújo, S. S., Pereira, M. S., Alves, R. B., Favaro, D. C., Hengge, A. C., Nagem, R. A. P., and Brandão, T. A. S. (2019) Catalytic mechanism for the conversion of salicylate into catechol by the flavin-dependent monooxygenase salicylate hydroxylase. *International Journal of Biological Macromolecules*. **129**, 588–600
22. Wierenga, R. K., Terpstra, P., and Hol, W. G. J. (1986) Prediction of the occurrence of the ADP-binding βαβ-fold in proteins, using an amino acid sequence fingerprint. *Journal of Molecular Biology*. **187**, 101–107
23. Eppink, M. H. M., Schreuder, H. A., and van Berkel, W. J. H. (1997) Identification of a novel conserved sequence motif in flavoprotein hydroxylases with a putative dual function in FAD/NAD(P)H binding. *Protein Science*. **6**, 2454–2458
24. Eppink, M. H. M., Overkamp, K. M., Schreuder, H. A., and van Berkel, W. J. H. (1999) Switch of coenzyme specificity of *p*-hydroxybenzoate hydroxylase. *Journal of Molecular Biology*. **292**, 87–96
25. Westphal, A. H., Tischler, D., Heinke, F., Hofmann, S., Gröning, J. A. D., Labudde, D., and van Berkel, W. J. H. (2018) Pyridine nucleotide coenzyme specificity of *p*-hydroxybenzoate hydroxylase and related flavoprotein monooxygenases. *Frontiers in Microbiology*. **9**, 1–17
26. Forneris, F., Orru, R., Bonivento, D., Chiarelli, L. R., and Mattevi, A. (2009) ThermoFAD, a Thermofluor®-adapted flavin ad hoc detection system for protein folding and ligand binding. *FEBS Journal*. **276**, 2833–2840
27. Romero, E., Gómez Castellanos, J. R., Gadda, G., Fraaije, M. W., and Mattevi, A. (2018) Same substrate, many reactions: oxygen activation in flavoenzymes. *Chemical Reviews*. **118**, 1742–1769
28. Mattevi, A. (2006) To be or not to be an oxidase: challenging the oxygen reactivity of flavoenzymes. *Trends in Biochemical Sciences*. **31**, 276–283
29. van Berkel, W. J. H., Benen, J. A. E., Eppink, M. H. M., and Fraaije, M. W. (1999) Flavoprotein kinetics. in *Flavoprotein Protocols* (Chapman, S. K., and Reid, G. A. eds), pp. 61–85, Humana Press, Totowa, NJ, 10.1385/1-59259-266-X:61
30. Sandro, G, and Massey, V (1989) Mechanisms of flavoprotein-catalyzed reactions. *European Journal of Biochemistry*. **181**, 1–17
31. Sucharitakul, J., Prongjit, M., Haltrich, D., and Chaiyen, P. (2008) Detection of a C4a-hydroperoxyflavin intermediate in the reaction of a flavoprotein oxidase. *Biochemistry*. **47**, 8485–8490
32. Nicoll, C. R., Bailleul, G., Fiorentini, F., Mascotti, M. L., Fraaije, M. W., and Mattevi, A. (2020) Ancestral-sequence reconstruction unveils the structural basis of function in mammalian FMOs. *Nature Structural and Molecular Biology*. **27**, 14–24
33. Krieger, E., Joo, K., Lee, J., Lee, J., Raman, S., Thompson, J., Tyka, M., Baker, D., and Karplus, K. (2009) Improving physical realism, stereochemistry, and side-chain accuracy in homology modeling: Four approaches that performed well in CASP8. *Proteins: Structure, Function and*

Downloaded from http://www.jbc.org/ at University of Groningen on September 15, 2020

*Bioinformatics*. **77**, 114–122
34. Entsch, B., and van Berkel, W. J. H. (1995) Structure and mechanism of *para*-hydroxybenzoate hydroxylase. *The FASEB Journal*. **9**, 476–483
35. Entsch, B., Cole, L. J., and Ballou, D. P. (2005) Protein dynamics and electrostatics in the function of *p*-hydroxybenzoate hydroxylase. *Archives of Biochemistry and Biophysics*. **433**, 297–311
36. van Berkel, W. J. H., Westphal, A., Eschrich, K., Eppink, M., and De Kok, A. (1992) Substitution of Arg214 at the substrate-binding site of *p*-hydroxybenzoate hydroxylase from *Pseudomonas fluorescens*. *European journal of biochemistry*. **210**, 411–419
37. Jadan, A. P., van Berkel, W. J. H., Golovleva, L. A., and Golovlev, E. L. (2001) Purification and properties of *p*-hydroxybenzoate hydroxylases from *Rhodococcus* strains. *Biokhimiya*. **66**, 1104–1110
38. White-Stevens, R. H., Kamin, H., and Gibson, Q. H. (1972) Studies of a flavoprotein, salicylate hydroxylse. I. Enzyme mechanism. *Journal of Biological Chemistry*. **247**, 2371–2381
39. Montersino, S., and van Berkel, W. J. H. (2012) Functional annotation and characterization of 3-hydroxybenzoate 6-hydroxylase from *Rhodococcus jostii* RHA1. *Biochimica et Biophysica Acta - Proteins and Proteomics*. **1824**, 433–442
40. Scrutton, N. S., Berry, A., and Perham, R. N. (1990) Redesign of the coenzyme specificity of a dehydrogenase by protein engineering. *Nature*. **343**, 38–43
41. Robinson, R., Franceschini, S., Fedkenheuer, M., Rodriguez, P. J., Ellerbrock, J., Romero, E., Echandi, M. P., Martin Del Campo, J. S., and Sobrado, P. (2014) Arg279 is the key regulator of coenzyme selectivity in the flavin-dependent ornithine monooxygenase SidA. *Biochimica et Biophysica Acta - Proteins and Proteomics*. **1844**, 778–784
42. Kamerbeek, N. M., Fraaije, M. W., and Janssen, D. B. (2004) Identifying determinants of NADPH specificity in Baeyer-Villiger monooxygenases. *European Journal of Biochemistry*. **271**, 2107–2116
43. Adam, W., Saha-Moller, C. R., Veit, M., and Welke, B. (1994) A convenient synthesis of hispidin from piperonal. *Synthesis*. **1994**, 1133–1134
44. Aliverti, A., Curti, B., and Vanoni, M. A. (1999) Identifying and quantitating FAD and FMN in simple and in iron-sulfur-containing flavoproteins. in *Flavoprotein Protocols* (Chapman, S. K., and Reid, G. A. eds), pp. 9–23, Humana Press, Totowa, NJ, 10.1385/1-59259-266-X:9
45. Bjellqvist, B., Hughes, G. J., Pasquali, C., Paquet, N., Ravier, F., Sanchez, J. -C., Frutiger, S., and Hochstrasser, D. (1993) The focusing positions of polypeptides in immobilized pH gradients can be predicted from their amino acid sequences. *Electrophoresis*. **14**, 1023–1031
46. Bjellqvist B, Basse B, Olsen E, C. J. (1994) Reference points for comparisons of two-dimensional maps of proteins from different human cell types defined in a pH scale where isoelectric points correlate with polypeptide compositions. *Electrophoresis*. **15**, 529–539
47. Lončar, N., Fiorentini, F., Bailleul, G., Savino, S., Romero, E., Mattevi, A., and Fraaije, M. W. (2019) Characterization of a thermostable flavin-containing monooxygenase from *Nitrincola lacisaponensis* (NiFMO). *Applied Microbiology and Biotechnology*. **103**, 1755–1764
48. Robert, X., and Gouet, P. (2014) Deciphering key features in protein structures with the new ENDscript server. *Nucleic Acids Res.* **42**, 320–324

Downloaded from http://www.jbc.org/ at University of Groningen on September 15, 2020

**Abbreviations and nomenclature**

| | |
|---|---|
| **McH3H** | hispidin 3-hydroxylase from *Mycena chlorophos* |
| **McLuz** | luciferase from *Mycena chlorophos* |
| **PTDH** | phosphite dehydrogenase |
| **$T_m$** | melting temperature |

Downloaded from http://www.jbc.org/ at University of Groningen on September 15, 2020

## Tables

**Table 1. Steady-state kinetics of McH3H and single mutants thereof.**
Steady-state kinetics analysis was carried out in the presence of 50 μM hispidin. The reaction was initiated by adding purified enzyme (25-100 nM). All reactions were performed in 50 mM potassium phosphate buffer, pH 7.0 at 25 °C.

| | NADH | | | NADPH | | | NADPH/NADH |
|---|---|---|---|---|---|---|---|
| Enzyme | $K_M$ (μM) | $k_{cat}$ ($s^{-1}$) | $k_{cat}/K_M$ ($s^{-1}mM^{-1}$) | $K_M$ (μM) | $k_{cat}$ ($s^{-1}$) | $k_{cat}/K_M$ ($s^{-1}mM^{-1}$) | ratio |
| WT | 240 ± 30 | 6.7 ± 0.2 | 28 ± 4 | 69 ± 11 | 6.0 ± 0.2 | 88 ± 20 | 3.2 |
| F44E | 22 ± 6 | 1.1 ± 0.1 | 50 ± 20 | 810 ± 180 | 2.5 ± 0.2 | 3.1 ± 1 | 0.062 |
| K45E | 44 ± 5 | 3.1 ± 0.1 | 71 ± 10 | 260 ± 38 | 4.7 ± 0.2 | 18 ± 4 | 0.25 |
| T46E | 200 ± 20 | 4.8 ± 0.2 | 25 ± 2 | 180 ± 20 | 6.3 ± 0.2 | 35 ± 5 | 1.4 |

Downloaded from http://www.jbc.org/ at University of Groningen on September 15, 2020

**Scheme**

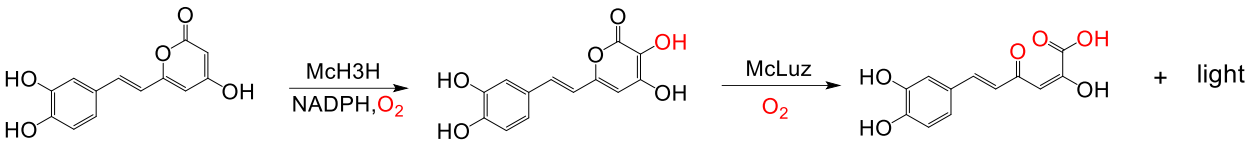


**Scheme 1. Bioluminescence process of fungi as catalyzed by McH3H and McLuz.**

Downloaded from http://www.jbc.org/ at University of Groningen on September 15, 2020

**Figures**

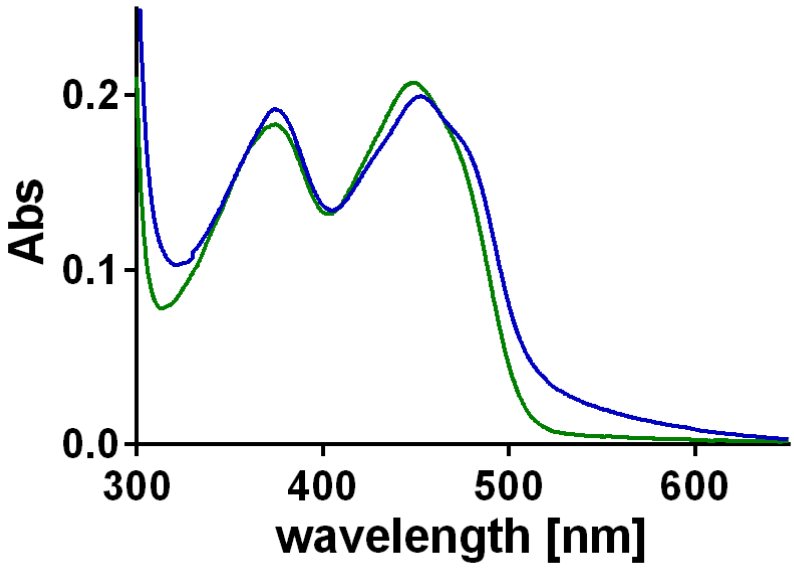


**Figure 1. UV-Vis absorption spectra of McH3H in 50 mM sodium phosphate, pH 7.0, 25 °C.**
McH3H native state: blue; unfolded McH3H (0.2% SDS): green.

Downloaded from http://www.jbc.org/ at University of Groningen on September 15, 2020

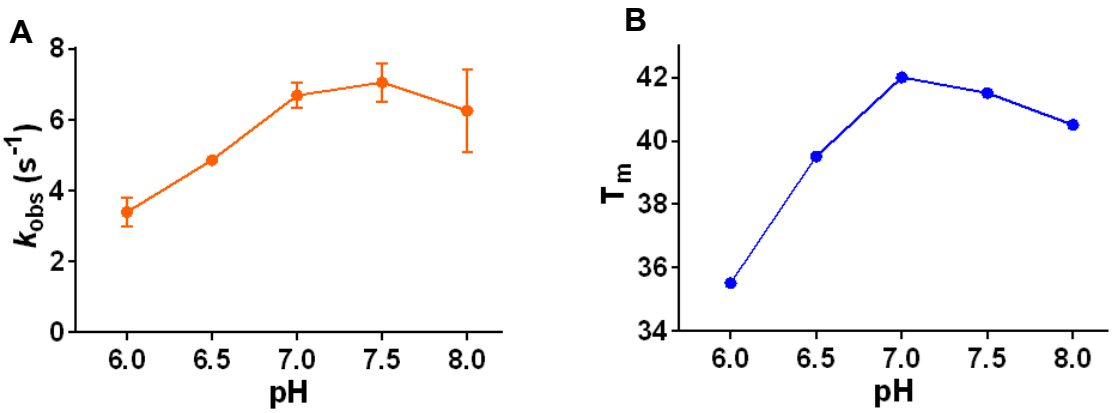


**Figure 2. Effect of pH on McH3H activity and thermal stability.**

Downloaded from http://www.jbc.org/ at University of Groningen on September 15, 2020

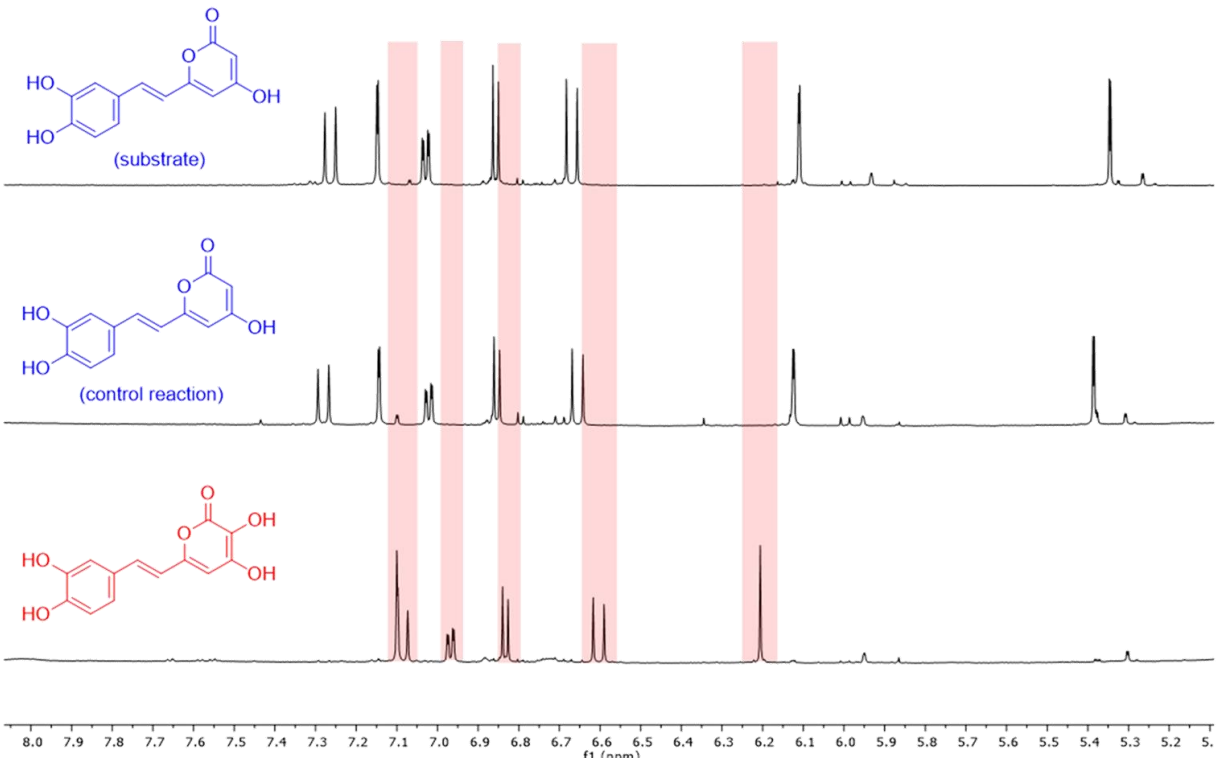


**Figure 3. $^{1}$H NMR spectra of hispidin and enzymatically synthesized 3-hydroxyhispidin.** The upper spectrum is a reference spectrum of hispidin, the middle spectrum was obtained upon incubating hispidin with an NADPH recycling system but no McH3H, while the lower spectrum was obtained when McH3H was present. Hispidin: (600 MHz, acetone-d6) δ 7.26 (d, J = 16.0 Hz, 1H), 7.15 (d, J = 2.1 Hz, 1H), 7.03 (dd, J = 8.2, 2.1 Hz, 1H), 6.86 (d, J = 8.2 Hz, 1H), 6.67 (d, J = 15.9 Hz, 1H), 6.11 (d, J = 2.0 Hz, 1H), 5.35 (d, J = 2.1 Hz, 1H); 3-Hydroxyhispidin: (600 MHz, acetone-d6) δ 7.11 – 7.07 (m, 2H), 6.97 (dd, J = 8.2, 2.0 Hz, 1H), 6.83 (d, J = 8.2 Hz, 1H), 6.60 (d, J = 16.0 Hz, 1H), 6.21 (s, 1H).

Downloaded from http://www.jbc.org/ at University of Groningen on September 15, 2020

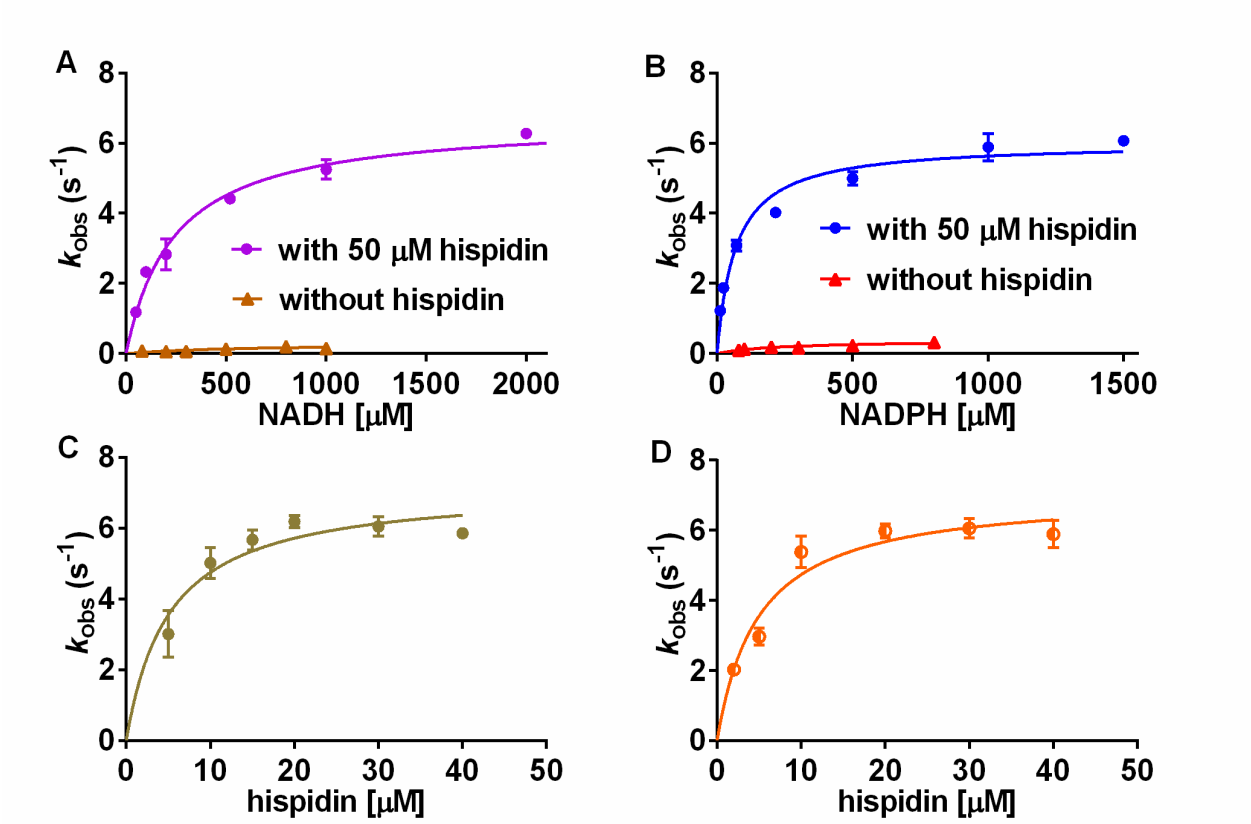


**Figure 4. Steady-state kinetics of McH3H.** (A) Steady-state kinetics on NADH in the presence and absence of 50 μM hispidin. (B) Steady-state kinetics on NADPH in the presence and absence of 50 μM hispidin. (C) Steady-state kinetics on hispidin in the presence of 3.0 mM NADH. (D) Steady-state kinetics on hispidin in the presence of 1.0 mM NADPH. The reaction was initiated by adding 25 nM purified enzyme. All reactions were performed in 50 mM potassium phosphate buffer, pH 7.0 at 25 °C.

Downloaded from http://www.jbc.org/ at University of Groningen on September 15, 2020

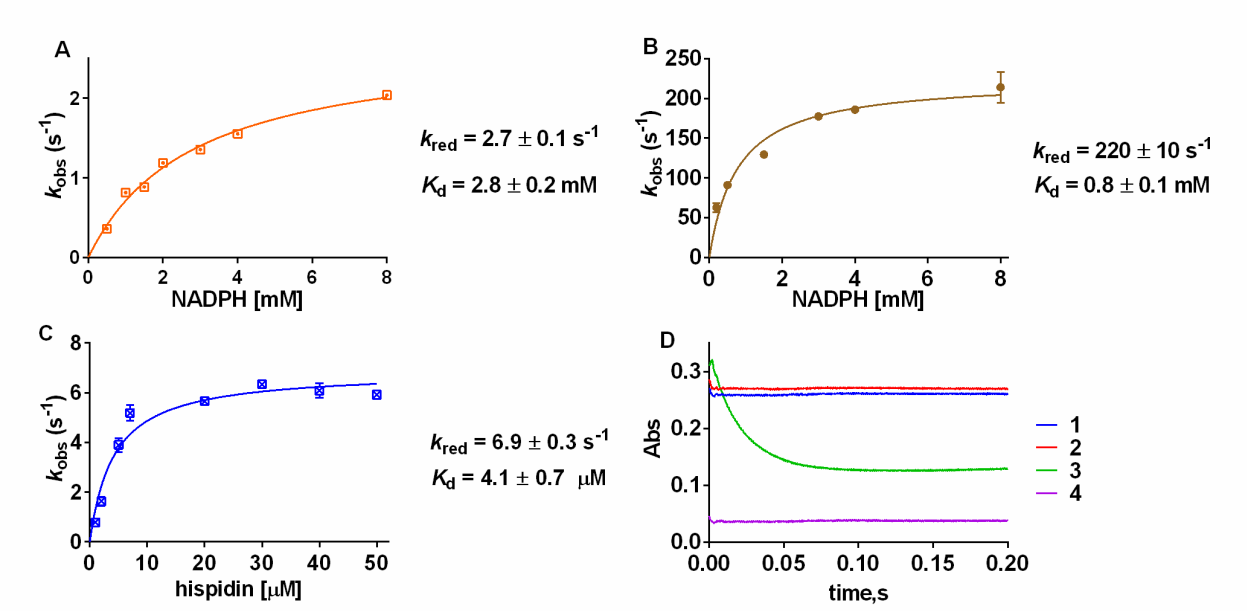


**Figure 5. Reductive half-reaction of McH3H.** (A) McH3H (10 μM) was anaerobically mixed with varying concentrations of NADPH. (B) McH3H (10 μM) was anaerobically mixed with varying concentrations of NADPH in the presence of 200 μM hispidin. (C) McH3H (2.5 μM) was anaerobically mixed with varying concentrations of hispidin and 20 μM NADPH. (D) Time course of absorbance changes at 450 nm of the enzyme in the presence of saturating concentrations of substrate (NADPH and/or hispidin) and atmospheric oxygen. Trace 1: 20 μM enzyme mixed with buffer; trace 2: 20 μM enzyme mixed with 500 μM NADPH; trace 3: 20 μM enzyme mixed with 200 μM hispidin and 500 μM NADPH; trace 4: absorbance of 200 μM hispidin. All reactions were performed in 50 mM potassium phosphate, pH 7.0 at 25 °C.

Downloaded from http://www.jbc.org/ at University of Groningen on September 15, 2020

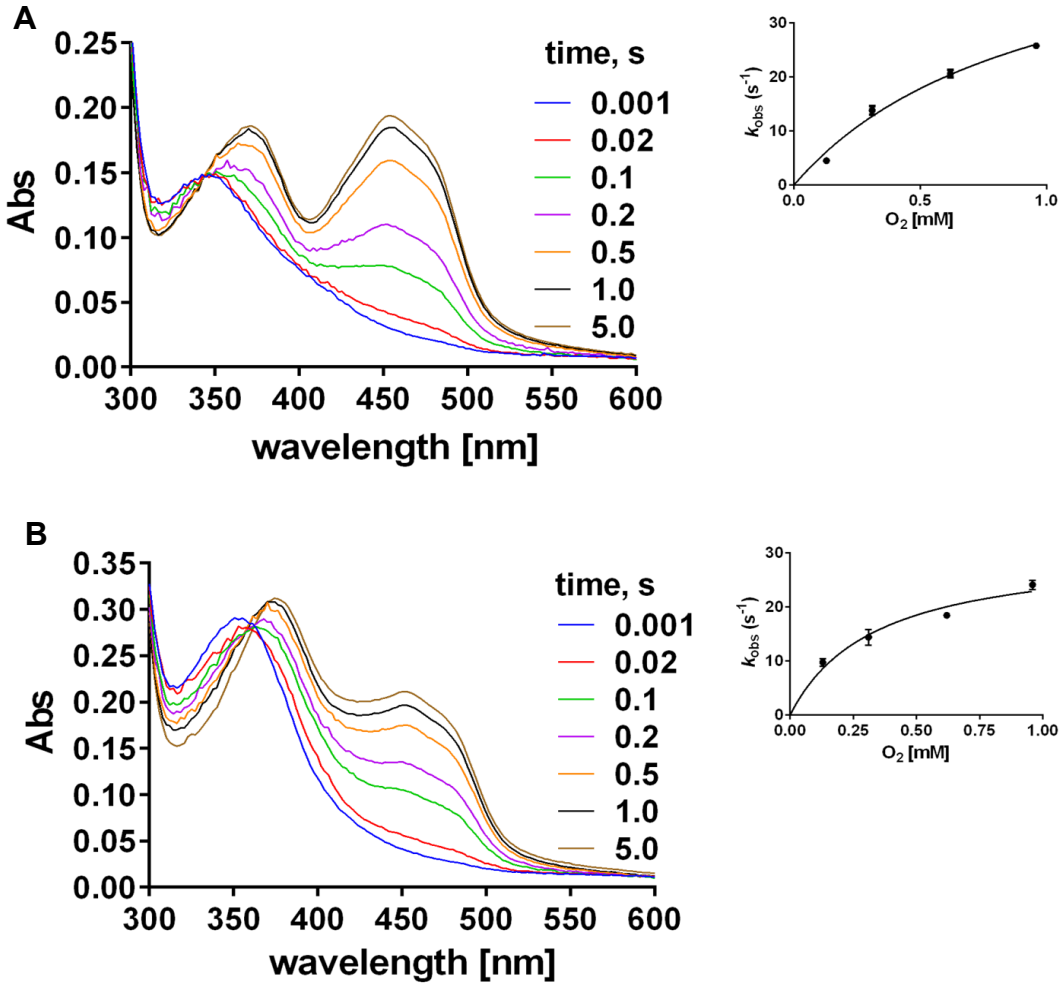


**Figure 6. Oxidative half-reaction of McH3H.** (A) NADPH-reduced McH3H (10 µM) was mixed with oxygen (130 µM). (B) NADPH-reduced McH3H (10 µM) was reacted with oxygen (130 µM) in buffer solution containing 10 µM hispidin. The insets show the observed rates of reoxidation at various $O_2$ concentrations as measured by (single exponent) fitting the absorbance increase at 375 nm. All reactions were performed in 50 mM potassium phosphate, pH 7 at 25 °C.

Downloaded from http://www.jbc.org/ at University of Groningen on September 15, 2020

**Substrate binding tunes the reactivity of hispidin 3-hydroxylase, a flavoprotein monooxygenase involved in fungal bioluminescence**

Yapei Tong, Milos Trajkovic, Simone Savino, Willem J.H. van Berkel and Marco W. Fraaije

*J. Biol. Chem. published online September 11, 2020*

---

Access the most updated version of this article at doi: 10.1074/jbc.RA120.014996

Alerts:
- When this article is cited
- When a correction for this article is posted

Click here to choose from all of JBC's e-mail alerts

Downloaded from http://www.jbc.org/ at University of Groningen on September 15, 2020